



## OPEN

## Single-channel multiplexing without melting curve analysis in real-time PCR

SUBJECT AREAS:  
PRECLINICAL RESEARCH  
MOLECULAR BIOLOGY

Young-Jo Lee, Daeyoung Kim, Kihoon Lee &amp; Jong-Yoon Chun

Seegene, Inc., Taewon Bldg., 91 Ogeum-ro, Songpa-Gu, Seoul 138-828, South Korea.

Received  
7 August 2014Accepted  
21 November 2014Published  
11 December 2014Correspondence and  
requests for materials  
should be addressed to  
J.-Y.C. (chun@  
seegene.com)

Multiplex real-time PCR with quantification of targets in a single fluorescence channel has been the demand in biotechnology industry. Here, we develop a novel analytical real-time PCR technique to detect multiple targets in a single fluorescence channel without melting curve analysis. In this technique, we show the intensity of the fluorescence signals of two discrete  $T_m$  targets is different at certain temperatures called detection temperatures, by which a high  $T_m$  target can be detected regardless of a low  $T_m$  target. We then identify the low  $T_m$  target by utilizing a change of the fluorescence signals between two different detection temperatures. Furthermore, it enables us to determine quantification of each target in a single channel, possibly facilitating convenient patient care for drug treatment in clinics.

The major advantage of real-time PCR is the development of homogeneous reactions, the amplification and detection of a target in real time<sup>1</sup>. As a result, real-time PCR has rapidly become the key tool for target and biomarker identification, expanding into applications as diverse as *in vitro* diagnostics (IVDs)<sup>2,3</sup>, food safety testing<sup>4,5</sup> and pharmacogenomics<sup>6,7</sup>.

However, the biotechnology industry has been struggling to meet the increasing demand for assays that provide both high-level multiplexing and quantification of targets using existing real-time PCR technologies<sup>8,9</sup>. To date, the industry has made considerable progress toward achieving these goals. For example, multiplex real-time PCR has been possible by using either multiple fluorescence channels or melting curve analysis after amplification<sup>10,11</sup>. In particular, the latter has been the best way to detect multiple targets in a single fluorescence channel. However, these methods still has several downsides, including crosstalk between channels, longer turnaround time (TAT) due to end-point analysis after the PCR step, and melting temperature ( $T_m$ ) variations<sup>12,13</sup>. Moreover, it is still impossible to obtain an individual  $C_t$  (threshold cycle) value of each of multiple targets in a single fluorescence channel.

To overcome these challenges, we develop a novel analytical technique, MuDT (Multiple Detection Temperatures), which enables us to detect multiple targets in a single fluorescence channel without melting curve analysis. To demonstrate how MuDT works, we employ TOCE (Tagging Oligonucleotide Cleavage and Extension)<sup>14</sup> technique to design oligonucleotides to detect the DNA target. TOCE utilizes indirect signal generation through the use of two novel components, Pitcher and Catcher. During each cycle, the Pitcher, a dual-purpose oligonucleotide that specifically binds to target DNA, is cleaved to release the unlabeled Extender that serves as a primer for an artificial template, a quenched-fluorescent molecule, the Catcher. Annealing and extension of the Extender on the Catcher generates Duplex Catcher, resulting in a fluorescence signal that is directly correlated to the quantity of the target DNA (Supplementary Fig. S1).

Overall, we verify that MuDT detects multiple targets in a single fluorescence channel. Notably, this method achieves  $C_t$  measurements for the targets, does not require melting curve analysis, and avoids crosstalk between channels; thus, MuDT has the potential to deliver more comprehensive and actionable diagnostics, leading to improved patient care and reduced healthcare costs.

## Results

**Intensity of the fluorescence signal depends on detection temperature.** During real-time PCR reaction, the duplex-driven fluorescence signal (designated as a yellow circle) of the probes depends on the temperature because of their melting curves (Fig. 1). Therefore, different intensities of those signals at certain temperatures at each cycle are able to detect the targets with different  $T_m$  values (highlighted in gray). These temperatures are defined as “detection temperatures” at which the intensity of a target’s fluorescence signal is measured.

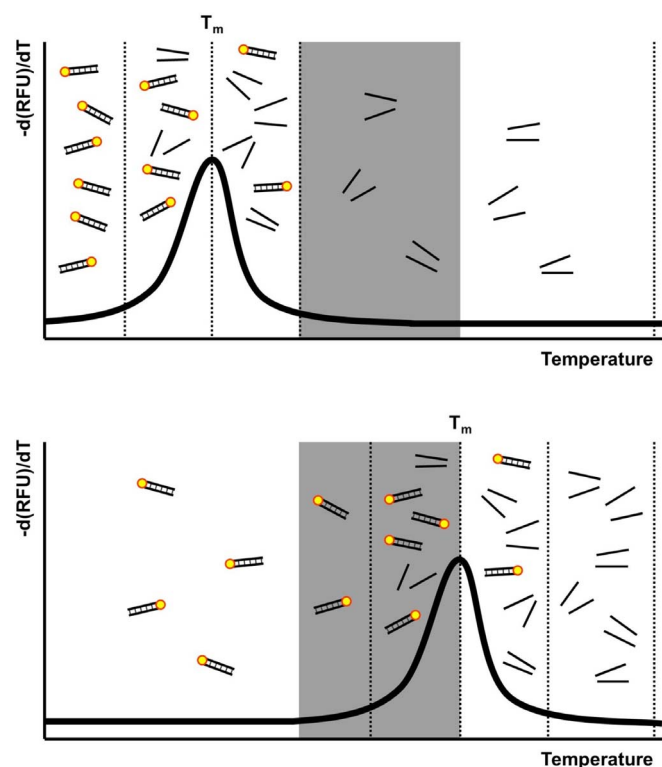


**Figure 1 | Intensity of the fluorescence signals depends on detection temperature.** Detection temperature means a certain temperature where the unquenched fluorescence signal is measured at each cycle during real-time PCR reaction. If there are two targets representing different  $T_m$  profiles, the fluorescence signals between two targets would be different at certain detection temperatures (marked in gray). Therefore, these temperatures differentiate the high  $T_m$  target from the low  $T_m$  target, by which the high  $T_m$  target can be detected.

Accordingly, the intensity of the fluorescence signals from the targets with different  $T_m$  profiles can be ascertained by controlling the detection temperatures in MuDT technique, enabling targets to be distinguished from each other without melting curve analysis.

**Identification of high  $T_m$  target by detection temperatures.** By using TOCE technique, we targeted the genomic DNA of two pathogens, *Chlamydia trachomatis* (CT)<sup>15</sup> and *Neisseria gonorrhoeae* (NG)<sup>15</sup>, with different  $T_m$  profiles, 75°C (high  $T_m$ ) and 65°C (low  $T_m$ ) respectively. We then confirmed that the designed components for targeting CT and NG yielded the unique and easily discernible  $T_m$  profiles (Fig. 2 and Supplementary Fig. S2). To demonstrate that detection temperatures control the intensity of fluorescence signals, we selected three different detection temperatures (60°C, 72°C, and 95°C). After annealing and extension at 60°C at each cycle, additional steps for detection (5 s each at 60°C, 72°C, and 95°C) were carried out and the outcomes were then compared. As expected, the fluorescence signals of both targets were vigorous at 60°C because this temperature is lower than their  $T_m$  values, insuring that fluorescence remains unquenched (Fig. 2a–b and Supplementary Fig. S2a–b). By contrast, no signal was detected for either target at 95°C due to fluorescence quenching at this temperature (Fig. 2a–b and Supplementary Fig. S2a–b). Importantly, we noticed that the two targets could be differentiated based on the dissimilar intensity of their unquenched fluorescence signals at a detection temperature of 72°C, at which the signal for NG was not detectable (Fig. 2a–b and Supplementary Fig. S2a–b).

These results prompted us to examine the signals at the same detection temperatures when both targets are present in the reaction. Under this condition, we observed the CT signal was also detected at

60°C and 72°C, strongly suggesting that CT (high  $T_m$  target) can be detected regardless of the presence of NG (low  $T_m$  target) (Fig. 2c and Supplementary Fig. S2c). Therefore, we concluded that the appearance of the fluorescence signal at a detection temperature at which no signal is detected for the low  $T_m$  target indicates the presence of the high  $T_m$  target. In addition, a  $C_t$  value of the high  $T_m$  target can be determined at this detection temperature.

**Detection of low  $T_m$  target by granting  $C_t$  value.** We next asked how the NG target with low  $T_m$  is recognized. To this end, we devised a novel analytical method that uses  $\Delta$ RFU (a change in Relative Fluorescence Units) of the targets between two different detection temperatures at each cycle during PCR reaction (Supplementary Fig. S3). So as to demonstrate this method, we first determined an arbitrary threshold that is defined as a minimum value over the  $\Delta$ RFU of the high  $T_m$  target between two different detection temperatures, ensuring cutting off the  $\Delta$ RFU value of the high  $T_m$  target. The determined threshold was then used to detect the low  $T_m$  target with its  $C_t$  value. For example, if both targets are present or the low  $T_m$  target is present alone,  $\Delta$ RFU between the two detection temperatures would be significantly higher than the determined threshold; thus, such a result would indicate the presence of the low  $T_m$  target. Subsequently, the  $C_t$  value of the low  $T_m$  target can be obtained from the amplification plot of the  $\Delta$ RFU of the low  $T_m$  target and the threshold eliminating the value of the high  $T_m$  target (designated by an arrow in Supplementary Fig. S3).

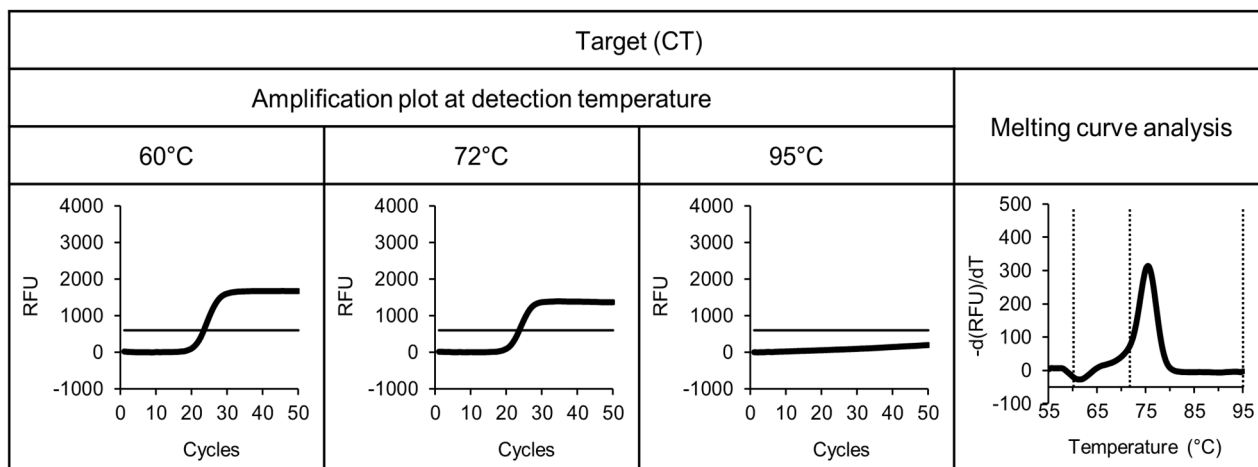
To test this idea, we plotted the  $\Delta$ RFU of the CT target between the two detection temperatures (60°C and 72°C) used in Figure 2 (Fig. 3a and Supplementary Fig. S4). A threshold was then determined by eliminating the  $\Delta$ RFU of the CT target. Indeed, the amplification plot was higher than the determined threshold when both targets were present or when NG was present alone (Fig. 3a and Supplementary Fig. S4). Using this information, we calculated a  $C_t$  value of the NG target from the cycle number at which the arbitrary threshold crossed the amplification plot (designated by an arrow in Fig. 3a and Supplementary Fig. S4).

To demonstrate that the obtained  $C_t$  value of the low  $T_m$  target (NG) correlates to its concentration, we plotted the  $\Delta$ RFU values of the NG target with serially diluted NG genomic DNA (1 ng–100 fg). As a result, we could measure different  $C_t$  values that certainly correlate to the concentration of NG gDNA (Fig. 3b, Supplementary Fig. 5a and 5b). We then evaluated the correlation coefficient ( $R^2$ ) to determine how well the data fit the standard curve. To this end, we plotted the  $C_t$  values against  $\log_{10}[\text{NG gDNA}]$  to obtain the amplification efficiency curve. The curve was linear across a 10<sup>5</sup>-fold range of input NG gDNA ( $R^2 > 0.99$ ), demonstrating that the  $C_t$  values of the low  $T_m$  target calculated with MuDT technique were directly correlated to the quantity of the target DNA, even when CT and NG were both present (Fig. 3b).

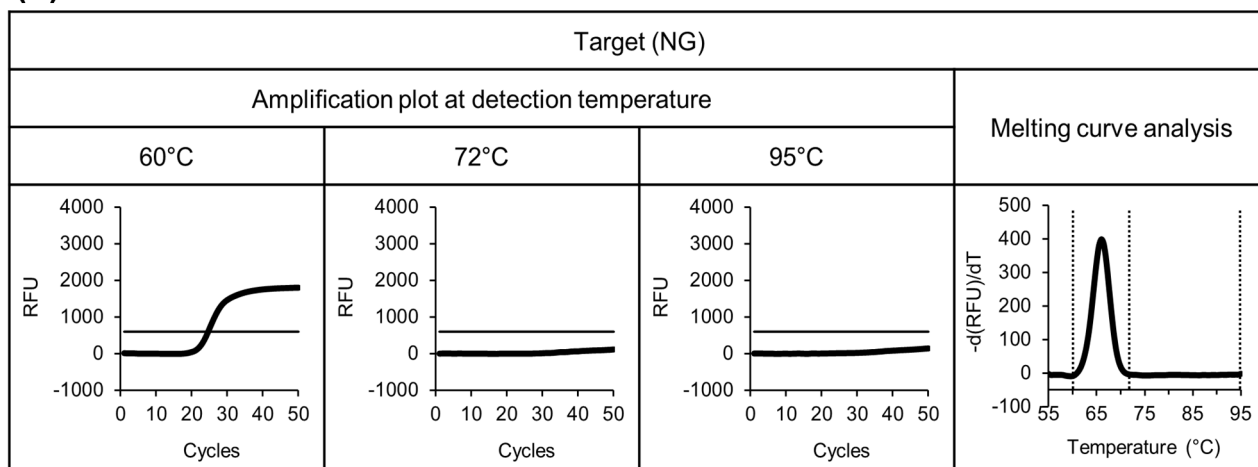
**Application of MuDT technique to detection of sexually transmitted infections in clinical samples.** To validate our result, we applied this technique to a commercially available Anyplex<sup>TM</sup> II STI-7 kit for detecting multiple pathogens in clinical specimens that cause sexually transmitted infections (STI)<sup>16</sup>. This kit is based on TOCE technique so that targets are detected by melting curve analysis. As shown in Table 1, it contains four channels each of which has two targets with different  $T_m$  values. To test whether MuDT can identify multiple pathogens in clinical samples by using this diagnostic product, we first selected two detection temperatures (72°C and 60°C). We then determined a respective arbitrary threshold from the  $\Delta$ RFU of high  $T_m$  targets between these two detection temperatures to discover each low  $T_m$  target. As a result, the different intensities of the fluorescence signals at 72°C enabled us to detect the high  $T_m$  targets in each channel with their own  $C_t$  value. We also acquired an individual  $C_t$  value of the low  $T_m$  targets in each



(a)



(b)



(c)

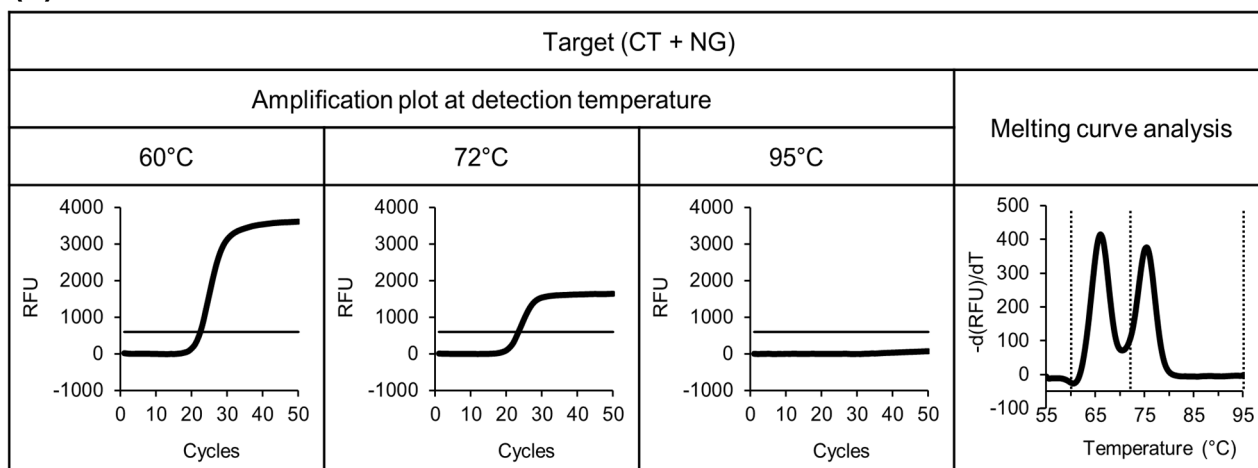
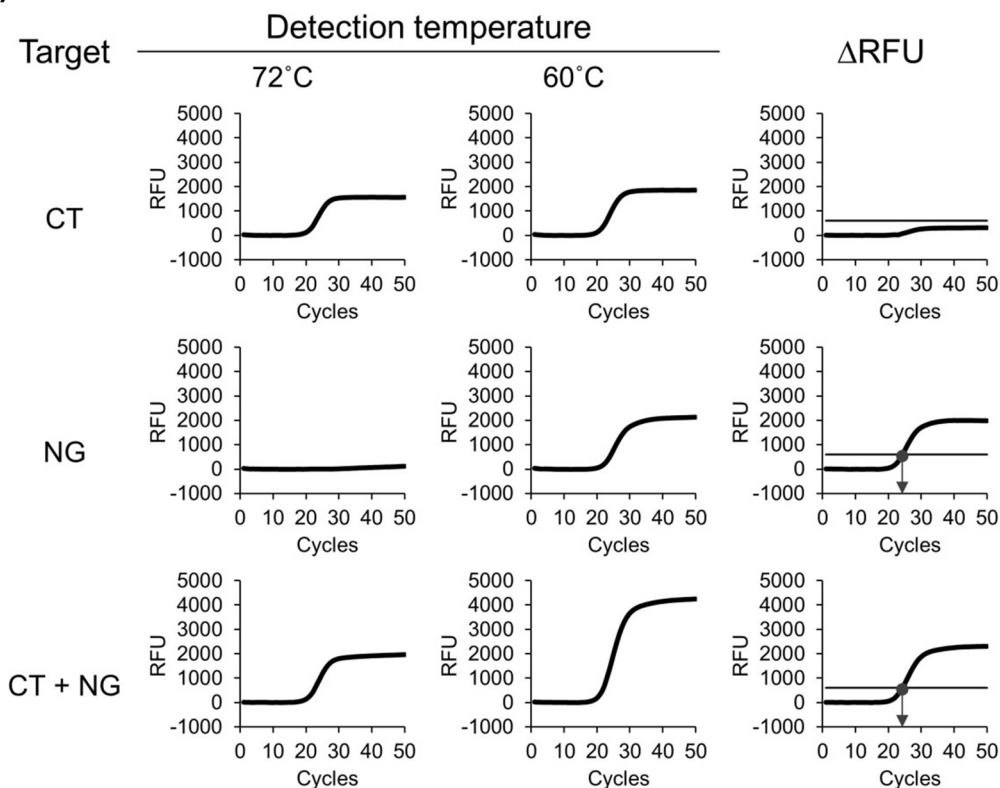


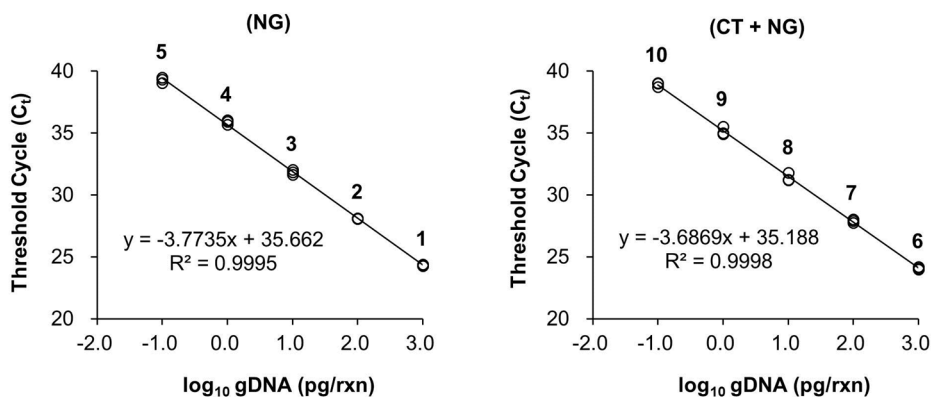
**Figure 2 | Identification of the high  $T_m$  target by detection temperatures.** (a) A Multiple Detection Temperature (MuDT) reaction was assembled for the screening of *Chlamydia trachomatis* (CT) (high  $T_m$ ), and the fluorescence signal was detected at three different detection temperatures (60°C, 72°C, and 95°C) at each PCR cycle. The first three graphs represent the amplification plots for the target, and the last graph contains the composite melting curves of the targets and three detection temperatures shown as dotted lines. (b and c) Procedures are the same as in (a), except that *Neisseria gonorrhoeae* (NG) (low  $T_m$ ) alone (b) or both targets (c) were screened.



(a)



(b)



No.		1	2	3	4	5	6	7	8	9	10
log <sub>10</sub> gDNA (pg/rxn)	CT	-	-	-	-	-	3	3	3	3	3
	NG	3	2	1	0	-1	3	2	1	0	-1

**Figure 3 | Detection of the low  $T_m$  target by granting a  $C_t$  value.** (a) The arbitrary threshold derived from the  $\Delta$ RFU of the high  $T_m$  target at two different detection temperatures was applied to calculate the  $C_t$  value of *Neisseria gonorrhoeae* (NG) (low  $T_m$ ), designated by an arrow. NTC is no-target control. (b) Calculation of the  $C_t$  values with a serial dilution of NG gDNA (1 ng–100 fg). Left panel: NG alone; right panel: both *Chlamydia trachomatis* (CT) (high  $T_m$ ) and NG. The averages (AVE) of the  $C_t$  values of three different experiments are shown.  $R^2$  indicates correlation coefficient, whereas the slope represents the efficiency of PCR.  $\Delta$ RFU represents the value deducted the RFU at 72°C from that at 60°C. The table shown represents the concentration of each reaction.



Table 1 | Application of MuDT technique to detection of sexually transmitted infections in clinical samples

Sample No.	Melting curve analysis								MuDT ( $C_t$ value)							
	Ch 1		Ch 2		Ch 3		Ch 4		Ch 1		Ch 2		Ch 3		Ch 4	
	UU	UP	MG	MH	NG	CT	IC	TV	UU	UP	MG	MH	NG	CT	IC	TV
1	+	+	ND	+	ND	+	+	ND	38.12	34.37	ND	38.33	ND	29.09	32.68	ND
2	+	ND	ND	ND	+	+	+	ND	39.53	ND	ND	ND	29.33	36.62	30.88	ND
3	ND	+	ND	+	ND	+	+	ND	ND	38.41	ND	27.02	ND	27.25	31.50	ND
4	+	+	ND	ND	+	ND	+	ND	34.87	28.24	ND	ND	28.88	ND	32.12	ND
5	+	+	ND	ND	ND	ND	+	ND	40.56	35.19	ND	ND	ND	ND	32.29	ND
6	+	+	ND	+	+	+	+	ND	38.25	35.53	ND	25.75	28.17	32.23	31.83	ND
7	ND	ND	+	ND	ND	ND	+	ND	ND	ND	44.04	ND	ND	ND	31.65	ND
8	+	+	ND	+	ND	+	+	ND	34.39	31.87	ND	28.86	ND	33.70	31.80	ND
9	ND	ND	ND	ND	+	+	+	ND	ND	ND	ND	ND	28.21	30.05	33.23	ND
10	+	+	ND	+	ND	+	+	ND	34.84	31.91	ND	28.17	ND	33.09	32.18	ND
11	+	ND	ND	ND	+	+	+	ND	37.09	ND	ND	ND	30.52	31.46	33.79	ND
12	ND	+	ND	+	+	+	+	ND	ND	44.84	ND	31.33	25.45	27.46	31.76	ND
13	+	ND	ND	ND	ND	+	+	ND	44.00	ND	ND	ND	ND	32.12	31.79	ND
14	ND	+	+	+	ND	+	+	ND	ND	37.71	33.57	25.45	ND	28.58	34.14	ND
15	ND	+	ND	ND	+	+	+	ND	ND	30.47	ND	ND	35.29	26.23	33.17	ND
16	+	+	ND	+	ND	ND	+	ND	41.55	40.66	ND	32.28	ND	ND	30.87	ND
17	+	ND	+	+	ND	+	+	+	31.63	ND	33.68	24.96	ND	26.63	31.68	44.73
18	+	+	+	+	ND	+	+	ND	40.06	48.41	38.66	31.11	ND	26.44	31.85	ND
19	+	ND	ND	ND	+	+	+	ND	41.39	ND	ND	ND	31.12	38.37	31.92	ND
20	+	ND	ND	ND	ND	+	+	ND	37.89	ND	ND	ND	ND	29.76	31.96	ND

Ch 1: Channel 1 (FAM);  
 Ch 2: Channel 2 (HEX);  
 Ch 3: Channel 3 (Cal Fluor Red 610);  
 Ch 4: Channel 4 (Quasar 670);  
 UU: *Ureaplasma urealyticum* (low  $T_m$ );  
 UP: *Ureaplasma parvum* (high  $T_m$ );  
 MG: *Mycoplasma genitalium* (low  $T_m$ );  
 MH: *Mycoplasma hominis* (high  $T_m$ );  
 NG: *Neisseria gonorrhoeae* (low  $T_m$ );  
 CT: *Chlamydia trachomatis* (high  $T_m$ );  
 IC: Internal control (low  $T_m$ );  
 TV: *Trichomonas vaginalis* (high  $T_m$ );  
 +: positive;  
 ND: not detected.

channel by using the determined thresholds (Table 1). These results confirm the capacity of MuDT in clinical diagnostics.

## Discussion

In this study, we demonstrated that MuDT is not a new type of oligo-based real-time PCR technique. Rather, it is a novel method for analyzing real-time PCR data, by which multiple targets are obviously detected in a single channel without melting curve analysis. Therefore, MuDT can apply its novel analytical method to any other hybridization-based chemistry<sup>17</sup> including molecular beacons<sup>18</sup>, FRET probes<sup>19</sup>, and any combination of these probes.

Moreover, MuDT technique opens the door for mingling with different fluorescence signal chemistries. Currently, hydrolysis- and hybridization-based chemistries are two major methods to generate fluorescence signal in real-time PCR. For instance, TaqMan probe uses the hydrolysis of the probe by 5' to 3' exonuclease activity of polymerase<sup>20</sup>, whereas TOCE is based on hybridization chemistry by which duplex formation of the Catcher generates fluorescence signal. We predicted that the use of a TaqMan probe in MuDT reaction enables us to design the targets with considerably high  $T_m$  value. Because the hydrolysis-based probe generates its fluorescence signal even at 95°C. However, the hybridized probe does not emit its signal at this temperature by denaturation of the probe (Fig. 2). Therefore, by using a TaqMan probe, it consequently ensures wider selection of detection temperatures, eventually detecting more targets in a single fluorescence channel. To demonstrate the applicability of TaqMan probe in MuDT, we tested a TaqMan probe as a target with high  $T_m$ . As a result, two targets with different fluorescence chemistries were also detected in a single channel (Supplementary

Fig. S6). This result confirmed the possible scenario for multiplexing for detection of more than two targets in a single channel in MuDT reaction.

In addition, MuDT will upgrade any real-time PCR instrument for more than double capacity of multiplexing without increasing number of channels demanding expensive costs, and to develop a universal single reagent (assay) without crosstalk between channels.

Clinically, co-infection of pathogens is dangerous to patients. Therefore, the necessary assay(s) should be multiplexing to detect all of them simultaneously and each target should be quantified as well. However, current real-time PCR chemistries are impossible to provide quantitative measurements for multiple targets in a single channel. Here, we probed that MuDT grants each  $C_t$  value to the targets in a single channel. Therefore, the multi-quantitation capability of this technique will enable clinicians to gain a complete package of diagnostic information including the diagnosis of disease, degree of disease progression and severity, and monitoring of treatment.

In conclusion, we achieved the longstanding goal for more than 20 years in real-time PCR systems by developing a novel target-detection technique. With these successful results, we anticipate that MuDT will generate convenient multiplexing with quantification, better assay system and easier patient care.

## Methods

**Preparation of target DNA.** Bacteria and genomic DNA [*Chlamydia trachomatis* (ATCC VR-1500) and *Neisseria gonorrhoeae* (ATCC 700825D)] were purchased from ATCC (VA, USA). DNAs extracted from swab and urine specimens were used for the detection of sexually transmitted infections. The QIAamp DNA Mini Kit (Qiagen, Germany) was used to purify genomic DNA.



**Designing of Oligonucleotides.** The oligonucleotide sequences used in this study are listed in Supplementary Table S1. Oligonucleotides were purchased from Integrated DNA Technologies Inc. (IA, USA) and Biosearch Technologies Inc. (CA, USA).

**MuDT reaction and melting curve analysis for the high  $T_m$  target.** Multiple Detection Temperature (MuDT) reactions were carried out in the final volume of 20  $\mu$ l containing 1 ng of each genomic DNA (CT or NG, or both), 10 pmol of each primer set (NG-F/NG-R and CT-F/CT-R), 5 pmol of each Pitcher (NG-P and CT-P1) and 1 pmol of each Catcher (NG-C and CT-C) in buffer containing 2 units of *Taq* DNA polymerase, 200  $\mu$ M of dNTPs and 2 mM of  $MgCl_2$ . The whole PCR steps are as follows: denaturation for 15 min at 95°C, and 50 cycles of denaturation (30 s at 95°C), annealing and extension (60 s at 60°C), and additional steps for detection (5 s each at 60°C, 72°C, and 95°C) in a CFX96 thermocycler (Bio-Rad, USA). Fluorescence signals were detected at three different detection temperatures (additional steps: 60°C, 72°C, and 95°C) at each cycle. Upon completion of the reaction, a melting curve was obtained by cooling the reaction mixture to 55°C, holding at 55°C for 30 s, and then increasing the temperature from 55°C to 95°C stepwise (0.5°C/step) with a 5 s hold between each step. Fluorescence was measured continuously during the temperature rises to monitor dissociation of double-stranded DNAs. Melting peaks were derived from the melting curve data (CFX96 Manager).

**MuDT reaction for the low  $T_m$  target.** MuDT reactions were carried out in the final volume of 20  $\mu$ l containing 1 ng of each genomic DNA (CT or NG, or both), 10 pmol of each primer set (NG-F/NG-R and CT-F/CT-R), 5 pmol of each Pitcher (NG-P and CT-P1) and 1 pmol of each Catcher (NG-C and CT-C) in buffer containing 2 units of *Taq* DNA polymerase, 200  $\mu$ M of dNTPs and 2 mM of  $MgCl_2$ . The whole PCR steps are as follows: denaturation for 15 min at 95°C, and 50 cycles of denaturation (30 s at 95°C), annealing (60 s at 60°C), and extension (30 s at 72°C) in a CFX96 thermocycler (Bio-Rad, USA). Fluorescence signals were detected at annealing step (60°C) and extension step (72°C) at each cycle.

**MuDT reaction for linearity of the low  $T_m$  target.** MuDT reactions were performed in a final volume of 20  $\mu$ l containing 1 ng of CT genomic DNA, serially diluted NG genomic DNA (1 ng–100 fg), 10 pmol of each primer set (NG-F/NG-R and CT-F/CT-R), 5 pmol of each Pitcher (NG-P and CT-P1), and 1 pmol of each Catcher (NG-C and CT-C) in buffer containing 2 units of *Taq* DNA polymerase, 200  $\mu$ M of dNTPs and 2 mM of  $MgCl_2$ . The whole PCR steps and detection of the fluorescence signals followed the same procedure as the MuDT reaction for detection of the low  $T_m$  target.

**MuDT reaction and melting curve analysis for detection of sexually transmitted infections.** Anyplex™ II STI-7 Detection (Catalog Number: SD7700Y, Seegene, Korea) was used for detection of sexually transmitted infections. Reactions were performed according to the protocol described by the product's manufacturer. Fluorescence signals were detected at annealing step (60°C) and extension step (72°C) at each cycle. Upon completion of the reaction, a melting curve was obtained by cooling the reaction mixture to 55°C, holding at 55°C for 30 s, and then increasing the temperature from 55°C to 85°C stepwise (0.5°C/step) with a 5 s hold between each step. Fluorescence was measured continuously during the temperature rises to monitor dissociation of double-stranded DNAs. Melting peaks were derived from the melting curve data (CFX96 manager).

**MuDT reaction using a TaqMan probe.** MuDT reactions were carried out in the final volume of 20  $\mu$ l containing 1 ng of each genomic DNA (CT or NG, or both), 10 pmol of each primer set (NG-F/NG-R and CT-F/CT-R), 5 pmol of Pitcher (NG-P), 1 pmol of Catcher (NG-C) and 1 pmol of TaqMan probe (CT-P2), in buffer containing 2 units of *Taq* DNA polymerase, 200  $\mu$ M of dNTPs and 2 mM of  $MgCl_2$ . The whole PCR steps and detection of the fluorescence signals followed the same procedure for the MuDT reaction for the low  $T_m$  target.

**Calculation of a  $C_t$  of the low  $T_m$  target.** During MuDT reactions, the fluorescence signal was observed at two different detection temperatures (60°C and 72°C) at each cycle. To obtain the  $C_t$  for the low  $T_m$  target, we first deducted the RFU at 72°C from the RFU at 60°C, and subtracted the calculated value by baseline. The  $\Delta$ RFU between the two detection temperatures (72°C and 60°C) was then plotted after selection of a suitable threshold, and then the  $C_t$  value was defined as the fractional cycle at which  $\Delta$ RFU reached the threshold level.

- Higuchi, R., Fockler, C., Dollinger, G. & Watson, R. Kinetic PCR analysis: real-time monitoring of DNA amplification reactions. *Biotechnology (NY)* **11**, 1026–1030 (1993).
- Espy, M. J. *et al.* Real-time PCR in clinical microbiology: applications for routine laboratory testing. *Clin Microbiol Rev* **19**, 165–256 (2006).

- Gunson, R. N., Collins, T. C. & Carman, W. F. Practical experience of high throughput real time PCR in the routine diagnostic virology setting. *J Clin Virol* **35**, 355–367 (2006).
- Hoorfar, J. Rapid detection, characterization, and enumeration of foodborne pathogens. *APMIS Suppl* **133**, 1–24 (2011).
- Maurin, M. Real-time PCR as a diagnostic tool for bacterial diseases. *Expert. Rev. Mol.Diagn.* **12**, 731–754 (2012).
- Postollec, F., Falentin, H., Pavan, S., Combrisson, J. & Sohier, D. Recent advances in quantitative PCR (qPCR) applications in food microbiology. *Food Microbiol* **28**, 848–861 (2011).
- Hiratsuka, M., Sasaki, T. & Mizugaki, M. Genetic testing for pharmacogenetics and its clinical application in drug therapy. *Clin. Chimica Acta* **363**, 177–186 (2006).
- Zhong, Q. *et al.* Multiple digital PCR: breaking the one target per color barrier of quantitative PCR. *Lab Chip* **11**, 2167 (2011).
- Settanni, L. & Corsetti, A. The use of multiplex PCR to detect and differentiate food- and beverage-associated microorganisms: a review. *J. Microbiol. Methods. Rev.* **69**, 1–22 (2007).
- Fu, G., Miles, A. & Alphey, L. Multiplex detection and SNP genotyping in a single fluorescence channel. *Plos One* **7**, e30340 DOI: 10.1371/journal.pone.0030340 (2012).
- Huang, Q. *et al.* Multiplex fluorescence melting curve analysis for mutation detection with dual-labeled, self-quenched probes. *Plos One* **6**, e19206 DOI: 10.1371/journal.pone.0019296 (2011).
- Whitell, D. M. & Sloots, T. P. Melting curve analysis using hybridization probes: limitations in microbial molecular diagnostics. *Pathol.* **37**, 254–265 (2005).
- Whitley, D. M., Mackay, I. M., Syrmis, M. W., Witt, M. J. & Sloots, T. P. Detection and differentiation of herpes simplex virus type 1 and 2 by a duplex LightCycler PCR that incorporates an internal control PCR reaction. *J. Clin. Virol.* **30**, 32–38 (2004).
- Lee, D. H. TOCE: Innovative Technology for High Multiplex Real-time PCR. *Seegene bulletin* **1**, 5–10 (2012).
- Low, A. J. *et al.* Neisseria gonorrhoeae and Chlamydia trachomatis infection in HIV-1-infected women taking antiretroviral therapy: a prospective cohort study from Birkinna Faso. *Sex Transm. infect.* **90**, 100–103 (2014).
- Choe, H. S. *et al.* Performance of Anyplex™ II multiplex real-time PCR for the diagnosis of seven sexually transmitted infections: comparison with currently available methods. *Int. J. Infect. Dis.* **17**, e1134–1140 (2013).
- Ranasinghe, R. T. & Brown, T. Fluorescence based strategies for genetic analysis. *Chem. Commun.* **44**, 5487–5502 (2005).
- Tyagi, S. & Kramer, F. R. Molecular beacons: probes that fluoresce upon hybridization. *Nature Biotech* **14**, 303–308 (1996).
- Witter, C. T., Herrmann, M. G., Moss, A. A. & Rasmussen, R. P. Continuous fluorescence monitoring of rapid cycle DNA amplification. *Bio Techniques* **22**, 130–138 (1997).
- Holland, P. M., Abramson, R. D., Watson, R. & Gelfand, D. H. Detection of specific polymerase chain reaction product by utilizing the 5' to 3' exonuclease activity of *Thermus aquaticus* DNA polymerase. *Proc. Natl. Acad. Sci.* **88**, 7276–7280 (1991).

## Acknowledgments

We thank In-Taek Hwang and Dae-Hoon Lee for critical reading of the manuscript. This work was supported by Seegene, Inc.

## Author contributions

Y.L., D.K. and K.L. performed the experiments. J.C. wrote the manuscript.

## Additional information

Supplementary information accompanies this paper at <http://www.nature.com/scientificreports>

**Competing financial interests:** The authors declare competing financial interests: patent application that is related to the research in this paper.

**How to cite this article:** Lee, Y.-J., Kim, D., Lee, K. & Chun, J.-Y. Single-channel multiplexing without melting curve analysis in real-time PCR. *Sci. Rep.* **4**, 7439; DOI:10.1038/srep07439 (2014).



This work is licensed under a Creative Commons Attribution-NonCommercial-NoDerivs 4.0 International License. The images or other third party material in this article are included in the article's Creative Commons license, unless indicated otherwise in the credit line; if the material is not included under the Creative Commons license, users will need to obtain permission from the license holder in order to reproduce the material. To view a copy of this license, visit <http://creativecommons.org/licenses/by-nc-nd/4.0/>